Available online at www.sciencedirect.com

ScienceDirect

Mendeleev Commun., 2024, **34**, 844–846

Mendeleev Communications

Impact of electron transport layer uniformity on field-induced degradation of inverted perovskite solar cells

Nikita A. Emelianov,*[a] Victoria V. Ozerova,[a] Anastasia A. Bizyaeva,[a,b] Mikhail S. Leshchev[a] and Pavel A. Troshin[c,a]

[a] *Federal Research Center of Problems of Chemical Physics and Medicinal Chemistry, Russian Academy of Sciences, 142432 Chernogolovka, Moscow Region, Russian Federation. E-mail: emelianov@icp.ac.ru*
[b] *D. I. Mendeleev University of Chemical Technology of Russia, 125947 Moscow, Russian Federation*
[c] *Zhengzhou Research Institute of HIT, Jinshui District, 450003 Zhengzhou, China*

DOI: 10.1016/j.mencom.2024.10.024

The impact of different electron transport layers (ETLs) based on fullerene derivatives, such as the well-known $PC_{61}BM$ and promising 3-pyridyl-substituted pyrrolidino[60]fullerene (PYF-30), on the electric field-induced degradation of inverted perovskite solar cells has been demonstrated. Devices assembled using PYF-30 and $PC_{61}BM$ deposited from deuterated chloroform exhibit significantly higher stability compared to $PC_{61}BM$ films deposited from chlorobenzene. The main reason for the decrease in the efficiency of the device during aging is the formation of pinhole-type defects in the ETL caused by the agglomeration of molecules of fullerene derivatives.

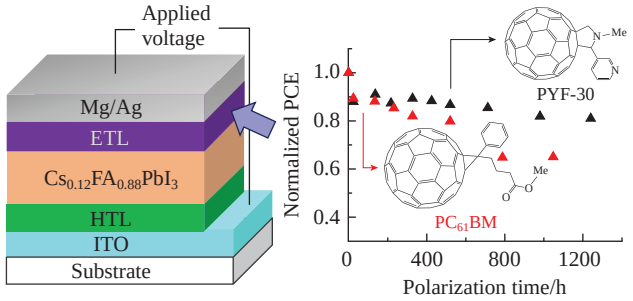

Keywords: pyrrolidinofullerenes, $PC_{61}BM$, electron transport materials, electric field-induced degradation, perovskite solar cells.

Fullerene derivatives currently represent the most widely used class of electron transport materials for perovskite solar cells (PSCs).[1,2] Their advantages include suitable energy levels that allow them to be used for efficient extraction of electrons from perovskite absorber materials, as well as low processing temperatures.[3] Nowadays, [6,6]-phenyl-C_{61}-butyric acid methyl ester ($PC_{61}BM$)[4,5] is one of the popular materials to form electron transport layers (ETLs) in inverted PSCs, which can achieve power conversion efficiency (PCE) of up to 25%. Unfortunately, this material forms non-uniform films with a significant number of defects.[6,7] The morphology of ETL films is crucial for achieving the required devices operational stability.[6] Furthermore, $PC_{61}BM$ is capable of absorbing and accumulating perovskite aging products such as methylamine, iodomethane, molecular iodine and hydrogen iodide.[7] Thus, to increase the device operational stability, it is necessary to introduce additional buffer layers.[8–10] Therefore, the search for new fullerene derivatives with both efficient charge carrier extraction and higher defect passivation capability than that of $PC_{61}BM$ is crucial for achieving simultaneously high efficiency and long-term operational stability of inverted PSCs.

Under operating conditions, PSCs are exposed to various factors that cause their degradation. The influence of external factors such as atmospheric oxygen and moisture can be successfully suppressed by encapsulation.[11] Hence, taking into account internal degradation processes under operating conditions is the key to understanding pathways to extend the service life of PSCs. Among them, the aging processes of charge transfer interlayers induced by an electric field have not been sufficiently studied, although they are the reasons for the accumulation of perovskite aging products and electrode corrosion.[6]

In this work, a systematic comparative study was carried out on the effect of fullerene derivative-based ETLs on electric field-induced aging of PSCs under well-controlled anoxic conditions. The following ETLs were used in the investigated devices: $PC_{61}BM$ films, deposited from solutions in chlorobenzene (PhCl) or deuterated chloroform ($CDCl_3$), and 3-pyridyl-substituted pyrrolidino-fullerene (PYF-30) films, deposited from a solution in carbon disulfide (CS_2). The use of different solvents to obtain $PC_{61}BM$ films is motivated by the fact that the solubility of fullerene derivatives and the rate of solvent evaporation strongly affect the film morphology[12] and, consequently, the operational stability of PSCs. Pyrrolidino[60]fullerenes synthesized by the authors' team were previously investigated as ETL materials in PSCs and showed attractive characteristics.[13] However, the operational stability of PSCs using pyrrolidinofullerene-based ETLs has not been studied.

Herein, PSCs were assembled in a p-i-n configuration, as shown in Figure 1. The ITO glass was coated with a hole transport layer (HTL) of poly[bis(4-phenyl)(2,4,6-trimethylphenyl)amine] (PTAA), which has previously demonstrated high resistance to electric field-induced aging.[14] Then, an absorber layer of double-cation perovskite $Cs_{0.12}FA_{0.88}PbI_3$, where FA denotes formamidinium cations $[CH(NH_2)_2]^+$, was deposited using an antisolvent quenching approach and coated with the corresponding ETL materials by spin-coating. $PC_{61}BM$ films were deposited from a 35 mg ml^{-1} solution in PhCl or a 30 mg ml^{-1} solution in $CDCl_3$. PYF-30 films were deposited from a 30 mg ml^{-1} solution in CS_2. The top Mg/Ag electrode was deposited by thermal evaporation in a vacuum through a shadow mask. Twelve devices of each type were fabricated and polarized. The graphs and table show the characteristics for the best samples.

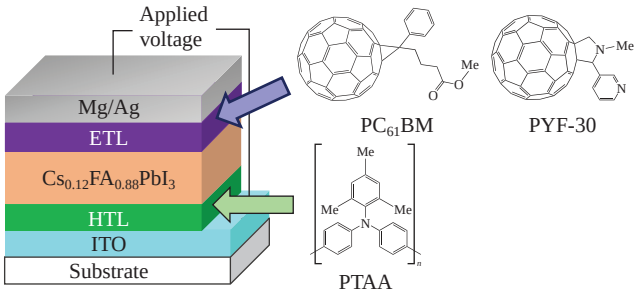

Figure 1 Schematic layout of the p-i-n PSC architecture used and the chemical structures of PYF-30 and $PC_{61}BM$ used in HTL and PTAA studied in ETL.

Electric field-induced aging experiments were performed in the dark at room temperature in a glove box with a well-controlled anoxic atmosphere (<0.1 ppm of O_2 and H_2O) to prevent interference with other stress factors. The measured initial V_{OC} values for the assembled PSCs with the ETLs investigated were 961–1015 mV (Table 1). Electric field-induced degradation of PSCs is greatly accelerated when the bias voltage becomes higher than the V_{OC} values of the devices.[15] Therefore, a bias voltage of 1.2 V was applied to accelerate the aging dynamics.

The ETL material was found to have a strong impact on the aging behaviour of devices, as shown in Figure 2. Devices with ETLs based on PYF-30 deposited from a solution in CS_2 and $PC_{61}BM$ deposited from a solution in $CDCl_3$ behave similarly, retaining more than 80% of the initial PCE value even after 1000 h of operation. While for PCSs with $PC_{61}BM$ deposited from a solution in PhCl, a rapid decrease in PCE was observed. Already after 400 h of exposure they lost up to 20% of the initial PCE, and after 800 h – up to 35%.

The decrease in efficiency of the $PC_{61}BM$_PhCl devices was also accompanied by a significant decrease in current density J_{SC} values, by almost a third, after 1000 h of bias exposure. This fact might be related to an increase in leakage currents in the devices, which could be caused by local point defects in the transport layers. FTIR microscopy mapping at 3271 cm^{-1}, corresponding to the N–H stretching vibration of the formamidinium cation,[16] was used to directly observe the structural defects in the thin films of the studied ETLs directly within the structure of PSCs after 1000 h of electric field-induced aging (Figure 3). This band was chosen to avoid overlap with the characteristic IR absorption peaks of the ETL materials (Figures S1 and S2, see Online Supplementary Materials). The bright areas observed on the scans correspond to regions with 'naked' perovskite, which unambiguously indicates the point defects within the ETL films. Such defects, called pinholes, lead to a direct contact of the perovskite with the top electrode, which has the most negative effect on the efficiency and stability of the fabricated perovskite solar cells.[17] In case of using $PC_{61}BM$ deposited from PhCl, the defect density was significantly higher compared to other samples (Figure 3). Thus, the formation of pinholes within the fullerene-based ETL correlates with a decrease in the device efficiency upon exposure to external bias.

Table 1 Characteristics of the inverted PSCs fabricated using fullerene derivatives as ETLs.

ETL material	Solvent for deposition	Scan direction	V_{OC}/mV	J_{SC}/ mA cm^{-2}	FF (%)	PCE (%)
$PC_{61}BM$	PhCl	Forward	957 ± 15	23.0 ± 0.2	69.3 ± 1.7	15.2 ± 0.8
		Reverse	957 ± 16	23.2 ± 0.4	69.0 ± 2.3	15.3 ± 0.7
$PC_{61}BM$	$CDCl_3$	Forward	980 ± 8	23.2 ± 0.0	73.7 ± 1.0	16.7 ± 0.6
		Reverse	977 ± 7	23.1 ± 0.3	73.5 ± 1.2	16.6 ± 0.7
PYF-30	CS_2	Forward	988 ± 59	23.4 ± 0.3	70.1 ± 0.8	16.1 ± 0.7
		Reverse	986 ± 53	22.9 ± 0.6	69.7 ± 1.0	15.8 ± 0.6

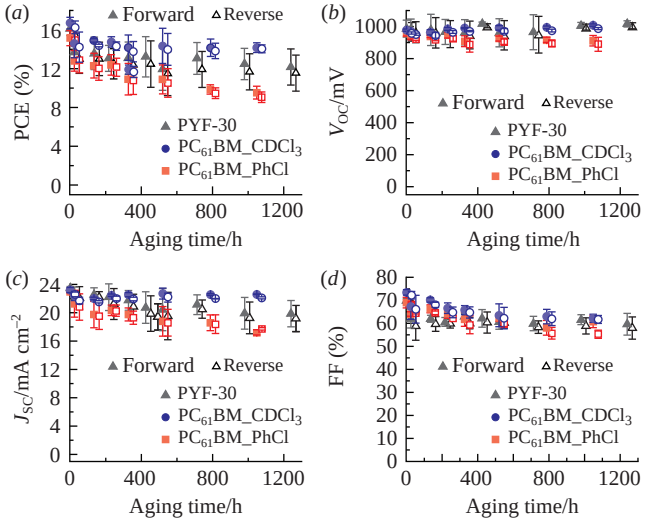

Figure 2 Degradation of the performance characteristics of PSCs upon exposure to a constant bias of 1.2 V: (*a*) PCE, (*b*) V_{OC}, (*c*) J_{SC} and (*d*) FF.

The morphology of the ETL films was also examined at the nanoscale using infrared scattering-type scanning near-field optical microscopy (IR s-SNOM) in order to better understand the nature of the pinhole formation process. For this purpose, the same surface area was scanned at the characteristic absorption frequencies of the perovskite absorber and the ETL material.[5] The characteristic absorption frequencies were chosen to avoid overlapping with the frequencies of another material (Figures S3 and S4). The resulting scans demonstrate a fundamental difference in the morphology of the ETLs (Figure 4). For $PC_{61}BM$ deposited from $CDCl_3$ and PYF-30, the film structure remained homogeneous, albeit with a few defects. On the contrary, for $PC_{61}BM$ deposited from PhCl, an intensive aggregation of fullerene derivative molecules was observed, thus leading to significant variations in thickness and local 'depths' exposing the perovskite surface. High phase contrast AFM scanning confirmed a significant difference in adhesion values for $PC_{61}BM$ deposited from PhCl (Figure S5).[18]

The reason for the observed aggregation may be the reorientation of the dipole moments of the side chains under the action of an external electric field.[19] Such different behaviour of $PC_{61}BM$ films formed from different solvents may be explained by the difference in the values of rotational diffusivity.[20] Thus, during the formation of a film from chlorobenzene, the molecules have a longer 'reaction rate' time to form a stable configuration and hence a dense film.

In conclusion, a systematic comparative study was carried out on the electric field-induced degradation of inverted PSCs assembled with the different fullerene-based ETLs. The devices with ETLs based on PYF-30 deposited from CS_2 and $PC_{61}BM$ deposited from $CDCl_3$ exhibited high stability even after exposure to a bias voltage of 1.2 V for 1000 h. In contrast, the most severe degradation was found for devices with a $PC_{61}BM$ layer conventionally deposited from PhCl. The marked difference in the degradation rate of PSCs directly correlated with the uniformity of the ETL

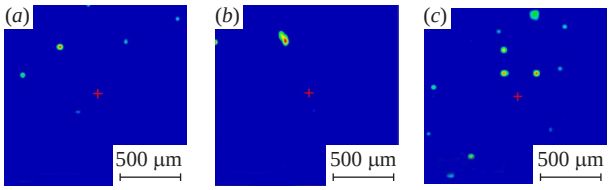

Figure 3 FTIR microscopy maps of ITO/PTAA/perovskite/ETL stacks with (*a*) PYF-30, (*b*) $PC_{61}BM$ (deposited from $CDCl_3$) and (*c*) $PC_{61}BM$ (deposited from PhCl) as ETL materials at the perovskite vibrational frequency (N–H stretching, 3271 cm^{-1}).

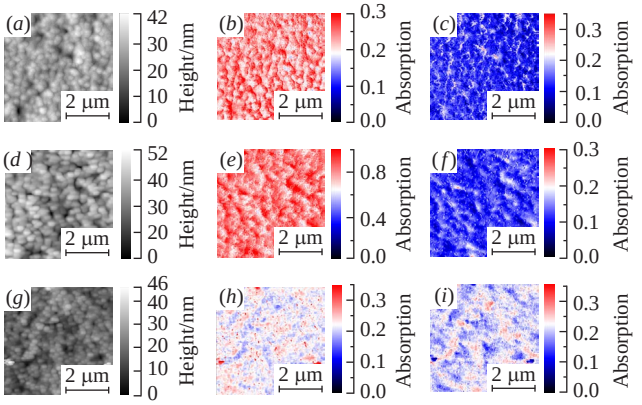

Figure 4 (*a*),(*d*),(*g*) AFM topography and (*b*),(*c*),(*e*),(*f*),(*h*),(*i*) IR s-SNOM maps at the characteristic frequencies of (*b*),(*e*),(*h*) ETL material (1026 cm^{-1} for PYF-30 and 1738 cm^{-1} for $PC_{61}BM$) and (*c*),(*f*),(*i*) perovskite (1047 cm^{-1}) for the films of (*a*)–(*c*) PYF-30, (*d*)–(*f*) $PC_{61}BM$ deposited from $CDCl_3$ and (*g*)–(*i*) $PC_{61}BM$ deposited from PhCl, which were formed on top of perovskite films.

film, in particular the density of pinhole defects identified by FTIR microscopy. It is especially noteworthy that IR s-SNOM measurements clearly demonstrated aggregation of $PC_{61}BM$ molecules in the films deposited from PhCl, which is the most plausible cause for poor film uniformity and defect formation.

This work was supported by the Russian Science Foundation (grant no. 22-73-00082).

Online Supplementary Materials

Supplementary data associated with this article can be found in the online version at doi: 10.1016/j.mencom.2024.10.024.

References

1 A. V. Mumyatov and P. A. Troshin, *Energy*, 2023, **16**, 1924; https://doi.org/10.3390/en16041924.
2 M. Ai, M. Chen and S. Yang, *Chin. J. Chem.*, 2023, **41**, 2337; https://doi.org/10.1002/cjoc.202300105.
3 L. Przypis, T. Ahmad, K. Misztal, D. Honisz, E. Radicchi, E. Mosconi, W. Domagala, F. De Angelis and K. Wojciechowski, *J. Phys. Chem. C*, 2021, **125**, 27344; https://doi.org/10.1021/acs.jpcc.1c07189.
4 Z. R. Sadretdinova, A. R. Akhmetov, R. B. Salikhov, I. N. Mullagaliev and T. R. Salikhov, *Mendeleev Commun.*, 2023, **33**, 320; https://doi.org/10.1016/j.mencom.2023.04.007.
5 Yu. G. Gorbunova, Yu. Yu. Enakieva, M. V. Volostnykh, A. A. Sinelshchikova, I. A. Abdulaeva, K. P. Birin and A. Yu. Tsivadze, *Russ. Chem. Rev.*, 2022, **91**, RCR5038; https://doi.org/10.1070/RCR5038.
6 E. M. Younes, A. Gurung, B. Bahrami, E. M. El-Maghraby and Q. Qiao, *Org. Electron.*, 2022, **100**, 106391; https://doi.org/10.1016/j.orgel.2021.106391.
7 M. M. Elnaggar, A. V. Mumyatov, N. A. Emelianov, L. G. Gutsev, V. V. Ozerova, I. V. Fedyanin, Y. V. Nelyubina, S. I. Troyanov, B. R. Ramachandran and P. A. Troshin, *Sustainable Energy Fuels*, 2023, **7**, 3893; https://doi.org/10.1039/D3SE00432E.
8 V. V. Ozerova, A. V. Mumyatov, A. E. Goryachev, E. A. Khakina, A. S. Peregudov, S. M. Aldoshin and P. A. Troshin, *Inorganics*, 2023, **11**, 153; https://doi.org/10.3390/inorganics11040153.
9 N. N. Udalova, N. N. Chertorizhskiy, E. N. Nemygina, A. V. Trubnikov, A. V. Kurkin, E. A. Goodilin and A. B. Tarasov, *Mendeleev Commun.*, 2023, **33**, 679; https://doi.org/10.1016/j.mencom.2023.09.028.
10 O. Fernandez-Delgado, P. S. Chandrasekhar, N. Cano-Sampaio, Z. C. Simon, A. R. Puente-Santiago, F. Liu, E. Castro and L. Echegoyen, *J. Mater. Chem. C*, 2021, **9**, 10759; https://doi.org/10.1039/D0TC05903J.
11 A. L. Montero-Alejo, F. Barría-Cáceres, L. Lodeiro and E. Menéndez-Proupin, *J. Phys. Chem. C*, 2023, **127**, 41; https://doi.org/10.1021/acs.jpcc.2c06499.
12 N. A. Belich, A. A. Petrov, P. A. Ivlev, N. N. Udalova, A. A. Pustovalova, E. A. Goodilin and A. B. Tarasov, *J. Energy Chem.*, 2023, **78**, 246; https://doi.org/10.1016/j.jechem.2022.12.010.
13 I. E. Kuznetsov, M. E. Sideltsev, V. G. Kurbatov, M. V. Klyuev and A. V. Akkuratov, *Mendeleev Commun.*, 2022, **32**, 527; https://doi.org/10.1016/j.mencom.2022.07.031.
14 P. A. Troshin, A. S. Peregudov, D. Mühlbacher and R. N. Lyubovskaya, *Eur. J. Org. Chem.*, 2005, 3064; https://doi.org/10.1002/ejoc.200500048.
15 A. V. Mumyatov, A. V. Chernyak, M. M. Elnaggar, P. M. Kuznetsov, A. F. Shestakov and P. A. Troshin, *Phys. Status Solidi RRL*, 2021, **15**, 2100181; https://doi.org/10.1002/pssr.202100181.
16 V. V. Ozerova, N. A. Emelianov, L. A. Frolova, Y. S. Fedotov, S. I. Bredikhin, S. M. Aldoshin and P. A. Troshin, *Sustainable Energy Fuels*, 2024, **8**, 997; https://doi.org/10.1039/D3SE01458D.
17 A. E. A. Bracesco, J. W. P Jansen, H. Xue, V. Zardetto, G. Brocks, W. M. M. Kessels, S. Tao and M. Creatore, *ACS Appl. Mater. Interfaces*, 2023, **15**, 38018; https://doi.org/10.1021/acsami.3c05647.
18 D. M. Montoya, E. Pérez-Gutiérrez, O. Barbosa-Garcia, W. Bernal, J.-L. Maldonado, M. J. Percino, M.-A. Meneses and M. Cerón, *Sol. Energy*, 2020, **195**, 610; https://doi.org/10.1016/j.solener.2019.11.098.
19 S. Sami, P. A. B. Haase, R. Alessandri, R. Broer and R. W. A. Havenith, *J. Phys. Chem. A*, 2018, **122**, 3919; https://doi.org/10.1021/acs.jpca.8b01348.
20 C. I. Wang and C. C. Hua, *J. Phys. Chem. B*, 2015, **119**, 14496; https://doi.org/10.1021/acs.jpcb.5b07399.

Received: 2nd May 2024; Com. 24/7484